iMag: Accurate and Rapidly Deployable Inertial Magneto-Inductive Localisation

Bo Wei[1], Niki Trigoni[2], and Andrew Markham[2]
[1]Teesside University, UK
[2]University of Oxford, UK
[1]b.wei@tees.ac.uk, [2]firstname.lastname@ox.ac.uk

***Abstract*— Localisation is of importance for many applications. Our motivating scenarios are short-term construction work and emergency rescue. Not only is accuracy necessary, these scenarios also require rapid setup and robustness to environmental conditions. These requirements preclude the use of many traditional methods e.g. vision-based, laser-based, Ultra-wide band (UWB) and Global Positioning System (GPS)-based localisation systems. To solve these challenges, we introduce *iMag*, an accurate and rapidly deployable inertial magneto-inductive (MI) localisation system. It localises monitored workers using a single MI transmitter and inertial measurement units with minimal setup effort. However, MI location estimates can be distorted and ambiguous. To solve this problem, we suggest a novel method to use MI devices for *sensing environmental distortions*, and use these to correctly close inertial loops. By applying robust simultaneous localisation and mapping (SLAM), our proposed localisation method achieves excellent tracking accuracy, and can improve performance significantly compared with only using an inertial measurement unit (IMU) and MI device for localisation.**

***Keywords*: Magneto-inductive device; Inertial measurements; Localisation; SLAM**

I. Introduction

This paper proposes iMag, an accurate, robust and fast setup Simultaneous Localisation and Mapping (SLAM) system. We aim to estimate the location of monitored people in challenging environments, i.e. areas where traditional RF or vision based systems fail or are not sufficiently robust. Personal localisation systems have a broad range of applications, such as emergency response [24], indoor location based service [33], [22] or construction site safety [27]. iMag uses inertial measurements for pedestrian dead reckoning, and uses Magneto-Inductive (MI) measurements for loop closure and correcting accumulated drift from inertial sensors. A key feature of our proposed method is the ability to drop a single transmitter in the area of interest and immediately start tracking. This is in stark contrast to other approaches e.g. Ultra-wideband (UWB) which need a large number of non-colocated anchors to be surveyed in place.

Motivating Scenario: short-term construction work. Official government reports indicate that workforce fatalities or injuries to railway workers occur due to insufficient warning when plant machinery or a train approaches [5], [6]. Here is an example scenario. Ten workers arrive at a railway construction site within a tunnel at 8:00 am. A localisation system needs to be set up to warn workers when they enter in a static danger zone or when their working area becomes a danger zone due to an incoming train. The plan is to commence work by 8:15 am, after a short site inspection. Many localisation techniques can achieve sub-metre accuracy, such as those using Global Positioning System (GPS) [12] , laser [9], camera [20] or UWB [11]. However, these techniques either require extensive site surveys and map-construction (e.g. UWB, camera, laser), or do not work well within enclosed areas like tunnels (e.g. GPS). The traditional method of ensuring track-worker safety is largely manual, through protection officers acting as a lookout and using the Autoprowa warning system [2], i.e. a light and horn, to warn construction workers. This needs additional labour, but more importantly, lookouts need to be alert for an entire shift. Furthermore, bad weather like fog also severely affects the lookout range of protection officers. GPS is popular for outdoor localisation applications [1], [4], but its positioning is only relatively accurate in very clear sky view. UWB is a promising technology for localisation with centimetre-level accuracy, but it is time consuming to deploy infrastructure. The basic principle behind UWB localisation is a triangulation method using range from receivers to transmitters. In other words, it requires multiple transmitters deployed on the field (at least 3 transmitters for 2D localisation or 4 transmitters for 3D localisation). In short-term construction work, installing and configuring an UWB localisation system is time-consuming and tedious. Obstacles, such as vegetation and machinery, can also easily attenuate UWB signals, limiting their use in these scenarios.

Fig. 1. Motivating scenario: short-term construction work (a) near a rail track (b) on road.

Many SLAM systems also fuse various types of measurements. Among them, camera-inertial and laser-inertial methods are popular and able to attain superior performance. However, both of them still have drawbacks. Bad weather (e.g. fog, rain and snow), low visual texture/features in

the surrounding environment (e.g. dust and muddy ground) and poor lighting conditions contrive to impact even the most sophisticated vision based localisation methods. Furthermore, dynamic environments, e.g. moving workers, can create difficulties for laser based applications. Lastly, vision and laser based techniques require the device to be worn for the duration of a shift in dusty conditions.

Magneto-Induction (MI) uses very low frequency (e.g. 2.5 kHz) that are generated at a transmitter. They have a number of key advantages over electromagnetic (RF, vision, laser) based techniques in that they allow through-obstacle localisation without requiring a line-of-sight connection [16]. In addition, as we use a triaxial transmitter and receiver, only a pair of devices is required to determine 3-D position and orientation. However, MI localisation systems are still *challenging* due to its difficulty of obtaining an accurate localisation estimate, especially at longer ranges. One localisation system [10] is proposed based on MI and inertial measurements, and it uses a particle filter for data fusion. However, it requires careful environmental surveying, i.e. time-consuming configuration for *each* MI transmitter/receiver pair and *each* specific environment. It is infeasible to exploit this method for rapidly deployable localisation.

We investigate an alternative and innovative method for using MI devices. *In our method, we no longer conduct environmental surveying. Instead, we leverage MI devices to sense environmental distortions and create unique spatially linked signatures. These unique features are used for loop-closure and calibrating biased pedestrian navigation trajectories from inertial measurements.* A robust SLAM framework is employed in order to improve localisation accuracy.

To summarise, the contributions of this paper are:

- We first propose an innovative method to enable a MI device to sense environmentally induced distortions. Spatial signatures are created by MI measurements to enable minimal effort for configuring MI devices. We take advantage of these features for loop closure and calibrating trajectories.
- We study the performance of MI estimates in typical environments, and demonstrate that MI measurements are highly jeopardised by ambiguity issues. We propose an inertial measurement based method to mitigate severe MI ambiguity issues.
- We propose the iMag SLAM system, which performs data fusion using MI and inertial measurements to achieve robust localisation with high accuracy.
- A prototype SLAM system has been implemented. Only one MI transmitter is deployed in the area of interest, which enables rapid setup. Extensive experiments are performed near a railway and at our campus to evaluate our proposed method.

The rest of this paper is organised as follows. Related work is demonstrated in Section II. Section III presents the system overview of our proposed localisation method. Section IV shows the details of the method using MI and inertial measurements for sensing environments and localisation. Evaluations are shown in Section V. Finally, we conclude this paper and present the future work in Section VI.

II. Related Work

In this section, we outline related research in three main areas: MI applications, high-resolution localisation, and wireless signal based localisation methods.

A. Magneto-Inductive Localisation

Recently, a number of MI-based devices have been designed for localisation. [18] designs a magnetic device for proximity detection for indoor applications. [25] uses MI-based signal to monitor the locations of underground animals. As the magnetic signal can penetrate soil and water, it achieves good accuracy and outperforms all other existing methods. [28], [29] also obtain an MI-based range first and then uses triangulation to estimate the location of monitored people.

We are not the first to apply inertial measurements with MI. [10] implements a 3-D inertial-MI system and performs data fusion using a simple particle filter model. They use inertial measurements along with the absolute positioning from MI signal, which needs careful calibration for each receiver-transmitter pair. On the contrary, our method takes advantage of the unique spatial features, so there is no need to have prior knowledge of a device and its operating environment.

B. High-resolution Sensor based Localisation Methods

There are many localisation systems based on high-resolution sensors, e.g. camera [20] and laser [9]. They can achieve centimetre accuracy in ideal conditions, but they have some key disadvantages that make them not particularly well suited to this application. Camera-based localisation is sensitive to poor lighting conditions, occlusions and dust. Similarly, laser based localisation is costly and can struggle with highly dynamic environments.

C. Wireless Signal Based Localisation Methods

WiFi signals are widely available in office and residential environments, and as a result, many solutions have been proposed for fusing WiFi and inertial measurements, such as [14], [15], [17]. However, WiFi is highly affected by multipath and would require a number of transmitters to be installed in the operating area. In addition, accuracy of WiFi based systems is typically in the 3-5 m region, due to variance in RSSI measurements and sensitivity to orientation and obstacles.

As an alternative spatially varying signal, the earth's magnetic field has been explored as a positioning modality. This is because it is influenced by ferrous objects in the surrounding environment, such as reinforcing steel inside buildings that distorts the earth's magnetic field. [32], [13], [26], [21], [31] combine these spatial features and inertial measurements for positioning. However, it is difficult to exploit these signatures in outdoor environment, where motion is less constrained and the signatures are less informative.

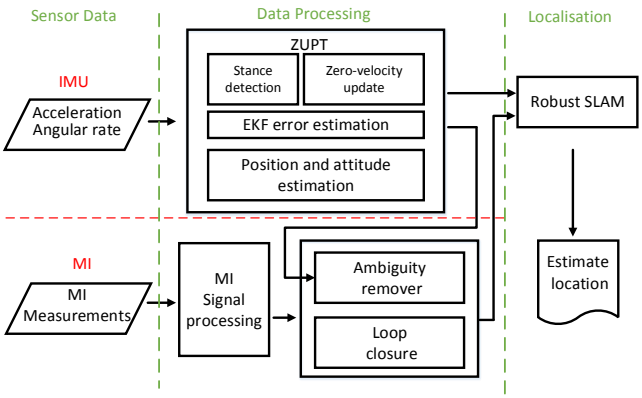

Fig. 2. System Flow Chart

UWB is an emerging state-of-the-art localisation infrastructure. It can achieve centimetre-level accuracy. With inertial measurements, it can track activity and gesture as well as localisation [30]. UWB does require a good transmitter geometry to be installed in the operating area, have a good line-of-sight, and the weak signals are easily blocked by obstacles and vegetation, impacting its robustness.

III. System Overview

To address the key challenges faced by teams of construction workers, the proposed system must satisfy the following three requirements:

- Localisation accuracy: workers must be positioned with metre level accuracy
- Robustness: the system must be immune to poor visual conditions and changes in the operating environment
- Rapidly deployable: the system must be easy to initialise to ensure low effort compliance and adoption

A system flow chart of our proposed localisation method is shown in Figure 2. Inertial measurements (i.e. acceleration and angular rate measurements) and MI measurements are first collected. Acceleration and angular rate come from a foot-mounted inertial measurement unit (IMU). A standard zero velocity update (ZUPT) [19] based tracker generates an inertial trajectory, which is subject to cumulative drift.

A single MI transmitter is placed in the Area of Interest, with each worker wearing a small MI receiver. The MI received signals are first cross-correlated with a reference template to extract the channel matrix. From the channel matrix and a standard physical model, a user's position is estimated. Note however, that this is typically incorrect due to distortions in the MI field. Furthermore, due to the long integration time (1 second in this case), motion induces random quadrant ambiguities i.e. x and y co-ordinates can be rotated by multiples of 90 degrees. It is clearly impossible to move from one side of the transmitter to the other in the matter of a second because of the dynamics of human motion, and thus these are first corrected with the aid of the inertial observations, giving rise to a distorted MI trajectory. This distorted trajectory is metrically compromised, but temporally stable and thus can serve as an indicator of loop closure. The loop closures from MI and the drifting inertial odometry are then passed into a Robust SLAM estimator to determine an accurate trajectory.

IV. Inertial Magneto-Inductive Localisation

In this section, we present the details of our proposed inertial magneto-inductive localisation system, iMag.

iMag uses a foot-mounted IMU, processed by the ZUPT algorithm. Overall, the performance of foot-mounted inertial navigation is good, but due to sensor noise and bias, the trajectory will slowly drift over time.

To overcome this cumulative drift, iMag uses MI measurements to detect loop closures and hence correct long-term errors in inertial odometry. An MI transmitter consists of three orthogonal coils which are tuned to resonance and are driven with a coded binary phase shift keying (BPSK) message. This code is chosen to have good cross-correlation properties, to increase the range of detectability. The MI receiver similarly consists of three orthogonal sensors (again coils in our case), which are connected to low noise amplifiers and a wide dynamic range ADC. The wide dynamic range is necessary to handle the high path-loss exponent - due to the near-field coupling, the field roll-off is 60 dB/decade, rather than the more typically encountered 40 dB/decade for electromagnetic propagation. The triaxial signals are then cross-correlated with the template code in order to estimate the channel matrix.

Once we have the channel estimates, we use the theory in [16], [10] to obtain 3-D position estimates[1]. Note however, that these position estimates are distorted by nearby ferrous objects. The distortions mainly cause arbitrary rotations of the position estimates. However, we note that these distortions are constant over time i.e. if the same point is revisited, then the same distorted position estimate will be obtained. It is this property that we aim to exploit to provide accurate long-term tracking.

However, before we use MI estimates for localisation or sensing environment, three issues have to be addressed: *(1) location distortion, (2) coordinate ambiguity, and (3) MI data association failure*. These arise mainly because of environmental noise, motion of the user, and the configuration of the MI system. Previous research [10] requires labour-expensive calibration of MI transmitter-receiver pairs to solve these issues for each environment. Rather than explicit calibration, we are the first to study the feasibility of exploiting these distortions to indirectly sense the operating environment and create spatially linked MI features.

To demonstrate some of the issues facing MI observations, we conduct an outdoor experiment to illustrate them.

We put one MI transmitter about 10 m away from the MI receiver, with a ground truth location of $(5.5, 9.1)$, as shown in Figure 3(a). Using the data process described in [10], we find MI estimates are ambiguous, i.e. locations are estimated

[1]The magnetic dipole equations are introduced in [16] and applied in [10] for 3-D localisation.

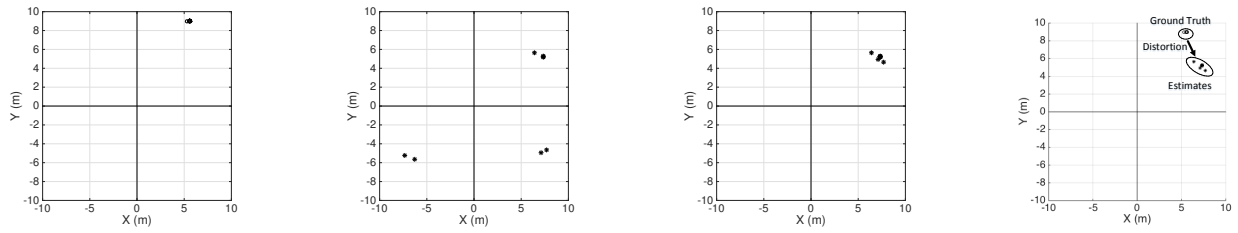

(a) (b) (c) (d)

Fig. 3. Experiment results showing MI issues (a) Ground truth. (b) Original MI estimates. (c) Optimised MI estimates using ambiguity remover (d) MI estimates showing distortion from ground-truth

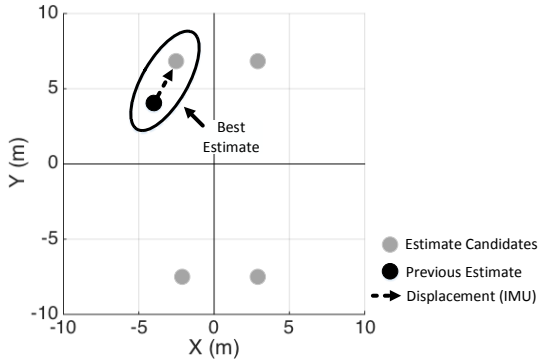

Fig. 4. An example of obtaining current MI location estimate

in different quadrants (shown in Figure 3(b)) instead of one. We thus propose a simple technique to remove quadrant ambiguity, as detailed below.

Coordinate Ambiguity Removal

One issue for the application of MI measurements is a quadrant coordinate ambiguity as shown in Figure 3(b). Theoretically, MI measurements should only be impacted by a hemispherical ambiguity. However, due to noise impacting the channel matrix pseudo-inverse, MI devices may still create ambiguous observations, especially when the height above ground is small. These quadrant ambiguities manifest as flips across the x axis or y axis.

To remove the coordinate ambiguity, additional knowledge needs to be provided. We propose to use an inertial trajectory based MI ambiguity remover. Its task is to find the maximum likelihood of the current i-th MI estimate $\hat{m}_i$ according to the previous estimate $\hat{m}_{i-1}$ and the displacement obtained from inertial measurements. Figure 4 shows an example of obtaining current MI location estimate from displacement calculated by inertial measurements and previous MI estimates. Specifically, the i-th MI estimate can be calculated by $\hat{m}_i = \arg\min_{m(c)_i} \|\hat{m}_{i-1} - m(c)_i\|_2$, where $m(c)_i$ is the i-th MI estimate in c-th quadrant.

We conduct a further experiment to illustrate its performance. The monitored person carries an MI receiver and walks in a square shape in an outdoor environment, stopping occasionally. The ground truth is shown in Figure 5(a), and Figure 5(b) depicts the original estimates. Without ambiguity removal, the MI observations are unusable as spatial features. After applying our proposed ambiguity remover, Figure 5(c) demonstrates a much cleaner trajectory. This shows the following observations: (1) our proposed method is able to sanitise MI observations; (2) this experiment further shows distortion of MI estimates even in outdoor environments; (3) MI signals generate unique spatial features - when the monitored person stops, MI estimates also deliver consistent estimates, as shown by the tight clustering of points.

Exploiting distorted locations

Instead of trying to overcome distortions and restore absolute MI positions, we simply accept that MI locations are not directly relatable to real-world co-ordinates through a pre-defined physical model. We consider MI estimates as observations in specific positions, termed as "*MI observations*", i.e. spatial features.

Even with the ambiguity removal method, obtained coordinates still do not match the ground truth, as shown in Figure 3(d). However, this observation also indicates another important fact, i.e. *even though MI estimates cannot determine the correct global location, they are unique to a specific location.* In other words, they have good discriminative power to indicate when a monitored person returns to the same point. Therefore, a single MI transmitter-receiver pair along with motion updates from inertial measurements are able to be used for accurate localisation, meeting the requirements of rapid deployment.

Loop-closure extraction

When a monitored person re-enters a known area, the current spatial features match previous ones stored in a map. The repeated MI observations can close an estimated trajectory loop and adjust the biased inertial trajectory.

Our MI devices have an update rate of approximately 1.4 Hz, which means it can obtain an estimate every approximately 0.7 second. The disadvantage of low sampling rate is two-fold. Firstly, the device rotation over this period can result in an incorrect MI channel estimation, due to the signal smearing between the axes, corrupting the channel matrix. Secondly, the collection density of the MI spatial features is low, i.e. we have sparse features to use as loop-closure keypoints. However, we note that the MI distortions lie on a smooth surface i.e. it is only large ferrous objects in the environment that can distort the MI field. The resultant field is an additive contribution from the MI source and the

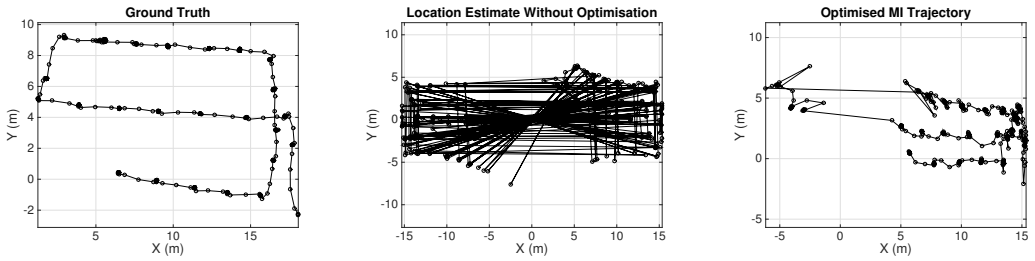

(a) (b) (c)

Fig. 5. Performance of MI ambiguity remover (a) Ground truth (b) Original MI estimates. (c) MI estimates after removing ambiguity.

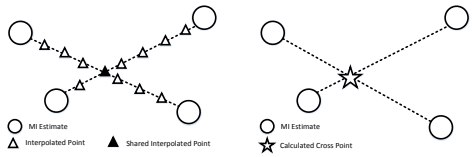

(a) (b)

Fig. 6. (a) Loop closure using interpolation method. (b) Loop closure using cross-point method

distorters.

Due to the smoothness of the location distortions, MI estimates can be interpolated by a linear model. A simple approach would be to upsample MI measurements into a denser grid, which would allow for more frequent loop-closure detections, as shown in Figure 6(a). Since the MI estimation rate is lower than inertial measurements, we can conduct linear interpolation for MI estimation, using the inertial measurement distance to distribute the points. An Euclidean distance threshold can be set to determine whether two points are in the same location or not, to detect potential loop-closures.

However, we propose a more computationally efficient method, which detects intersections of two line segments whose end points are neighbouring MI estimates, and we call this "cross-point" method. We use a curve intersection detection method in [3], as shown in Figure 6(b) .

Here we present the details of this method. We have two line segments M_i and M_j (obtained from inertial trajectories) with end points which are neighbouring MI estimates. The end points of M_i and M_j are $(m_i(1), m_i(2))$, $(m_{i+1}(1), m_{i+1}(2))$ and $(m_j(1), m_j(2))$, $(m_{j+1}(1), m_{j+1}(2))$ respectively. There are four unknowns here $d1$, $d2$, x_0 and y_0. (x_0, y_0) is the intersection point. $d1$ and $d2$ are the distance between starting points and intersection points relative to the length of two segments. The relation among these variables are shown in the simultaneous equations in Equation (1).

$$\begin{cases} (m_{i+1}(1) - m_i(1)) \times d1 = x_0 - m_i(1) \\ (m_{i+1}(2) - m_i(2)) \times d1 = y_0 - m_i(2) \\ (m_{j+1}(1) - m_j(1)) \times d2 = x_0 - m_j(1) \\ (m_{j+1}(2) - m_j(2)) \times d2 = y_0 - m_j(2) \end{cases} \tag{1}$$

In matrix form, we have $A \times U = B$, where A, U and B are shown in Equation (2), Equation (3) and Equation (4). U is the unknown matrix, and can be solved by $U = B \setminus A$.

$$A = \begin{bmatrix} m_{i+1}(1) - m_i(1) & 0 & -1 & 0 \\ 0 & m_{i+1}(2) - m_i(2) & -1 & 0 \\ m_{j+1}(1) - m_j(1) & 0 & 0 & -1 \\ 0 & m_{j+1}(2) - m_j(2) & 0 & -1 \end{bmatrix} \tag{2}$$

$$U = \begin{bmatrix} d1 & d2 & x_0 & y_0 \end{bmatrix}^T \tag{3}$$

$$B = \begin{bmatrix} -m_i(1) & -m_i(2) & -m_j(1) & -m_j(2) \end{bmatrix}^T \tag{4}$$

After solving the equation, we need to check $d1$ and $d2$ to find if these two line segments have an intersection or not. If both $d1$ and $d2$ are between 0 and 1, it means these two line segments intersect, and (x_0, y_0) is the intersection point.

The key advantage of the cross-point method is that it is approximately an order of magnitude faster than dense interpolation. This is important for a real-time localisation system, especially when a large number of candidate loop-closure points are being searched.

Map-building

Our system uses a robust GraphSLAM optimiser g2o [23]. This robust optimiser considers two joint parts for optimisation from odometry and loop closing constraints respectively. Scaling factors for information matrices are added to the loop closing constraints to increase robustness to outliers.

V. Evaluation

In this section, we evaluate the performance of our proposed iMag.

We perform experiments near a railway (Experiment 1 shown in Figure 7(a)) as well as at our campus, an outdoor environment with little vegetation (Experiments 2&3 shown in Figure 7(b)). Both of the experimental areas are a 40 m $\times$ 40 m open space. The reason we conduct experiments at our campus is the availability of the RTK GPS [12] signal, which is used for recording ground truth. Alongside the railway line, we found that RTK GPS coverage was patchy.

The goal of our experiments is to localise the monitored person and evaluate the accuracy of our proposed methods. We compare our proposed *iMag* with localisation methods only using *IMU* or *MI*. The following metrics are used in the experiments: (1) *Cumulative distribution function (CDF)*: The CDF of an error is a function whose value is the possibility that a corresponding estimate is less than or equal to the

(a) Alongside Railway

(b) Campus

(c) Hardware (Tx and Rx are short for transmitter and receiver respectively)

Fig. 7. Experimental Setup

argument of that error; (2) *Root Mean Square Error (RMSE)*: (e_{rms}) is the mean tracking error over the entire trajectory, defined as $e_{rms} = \sqrt{\frac{1}{t_e - t_s}\Sigma_{t=t_s}^{t_e}\hat{e}(t)^2}$. $\hat{e}(t)$ is the localisation error for time t, expressed as $\hat{e}(t) = \|\hat{l}(t) - l_g(t)\|$, where $\hat{l}(t)$ and $l_g(t)$ are estimates and ground truth, respectively.

A. Hardware for Localisation

In this section, we describe the hardware we use for experiments. Our prototype includes a laptop, an MI transmitter, an MI receiver, and an IMU as shown in Figure 7(c). An RTK GPS is also used for recording ground truth, which can achieve 10 cm accuracy with a clear sky view.

In our prototype, a laptop is carried by the monitored person to collect and process measurements. It has an Intel Core i7 with 2.8 GHz processor and 16 GB Memory. The operating system is Ubuntu 14.04.

The MI transmitter includes a 40 cm plastic cube former which has three mutually orthogonal coils. Each coil is 25 turns of 1 mm diameter enamelled copper wire. Powered by a 1.2 Ah 12 V battery, three H-bridges amplify the modulated BPSK signals generated by an STM32F4 microcontroller. The message is modulated at a rate of 31.25 bps. The transmitter operates at a nominal centre frequency of 2.5 kHz.

Similar to the MI transmitter, the MI receiver also equips a 10 cm plastic cube former wrapped by three mutually orthogonal coils of 150 turns/0.5 mm diameter enamelled copper wire. An ADS1274I 24 bit ADC is used for digitising received signals. An STM32F4 micro-controller then processes the digital signals, dropping them down to baseband and performing carrier wiping and phase recovery. A USB cable is used to connect the MI receiver to the laptop in order to transfer collected data and power the MI receiver.

The IMU we employ is the development board Xsens MTi-3-8A7G6-DK [8]. In our system, it continuously supplies inertial measurements, i.e. acceleration and angular rate, both at 100 Hz. The IMU is firmly mounted on one foot of a monitored person, and the inertial measurements are ported to the laptop through a USB cable for further processing.

B. Experiment 1: Feature stability

We perform this experiment to show the feasibility and efficacy of our proposed cross-point loop closure method using MI observations. This experiment is conducted near the railway line as shown in Figure 7(a), where significant quantities of metal (i.e. a train, a railway track and a transformer box) are nearby. This experiment also aims to show the ability to find unique MI spatial signatures in a metal-rich environment.

TABLE I
LOCALISATION ERROR OF EXPERIMENT 1

Method	IMU	MI	iMag
e_{rms}	4.384	2.634	1.330

We collect MI signals with the monitored person walking in a "cross" shape as shown in Figure 8(a)[2]. To stretch our proposed method to the limit, we synthesize a badly biased IMU trajectory (see Figure 8(b)). In a 70 m path, the end heading bias of our synthetic trajectory is approximately 12°, which is almost 5× more than the bias of a normal IMU [7].

Figure 8(c) demonstrates the MI observations after removing their ambiguity. Note how distorted the MI trajectory is. Although it broadly resembles the ground truth, it is compressed vertically and exhibits significant perturbations from a straight line. However, when the user re-enters a previous place (i.e. the origin), the MI observations are correctly able to extract loop-closures, resulting in the corrected SLAM trajectory in Figure 8(d). Table I shows that the e_{RMS} of IMU, MI and iMag method are 4.384 m, 2.634 m and 1.330 m, respectively. Fusing measurement from MI and IMU, iMag can achieve 69.6% and 49.5% improvement compared with IMU and MI based localisation methods. Figure 8(e) shows the CDF of errors using different methods. The results show the 80th percentile localisation errors for IMU, MI and iMag methods are 6.3 m, 3.1 m, and 1.5 m. In this metric, iMag achieves 76.2% (compared with the IMU method) and 51.6% (compared with the MI method) improvement.

This demonstrates that distorted MI observations are stable and unique in metal-rich environments, and have excellent discriminative power for loop-closure. The following experiments were conducted in an open outdoor space where the RTK GPS signal is available, and the inertial trajectory comes from a foot-mounted IMU. Note however, that even though these experiments were conducted in an open area, there were metallic pipes and wires underneath the experi-

[2]Because this area is too close to a train and a transformer box, the RTK GPS signal is missing in the experiment. Therefore, we manually label the ground truth for this experiment.

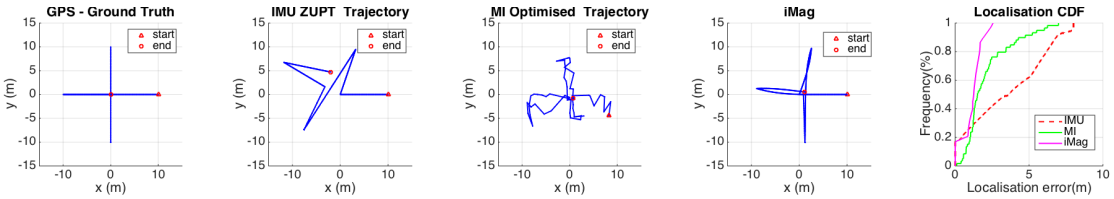

(a) Ground Truth (b) Synthetic highly biased IMU (c) MI (d) iMag (e) cdf

Fig. 8. Experiment 1: Trajectories and CDF along railway line

TABLE II
LOCALISATION ERROR OF EXPERIMENT 2

Method	IMU	MI	iMag
e_{rms}	4.527	4.247	0.752

TABLE III
LOCALISATION ERROR OF EXPERIMENT 3

Method	IMU	MI	iMag
e_{rms}	3.491	4.564	2.4532

mental area.

C. Experiment 2: Loop Closure Robustness

The goal of this experiment is to evaluate the robustness of MI observations to determine loop-closure points. The path includes numerous repeated MI observations that will lead to a large number of loop-closures as shown in Figure 9(a). During this experiment, the monitored person is walking in a square, which leads a 233.13 m path.

Figure 9(b) and Figure 9(c) demonstrate the IMU trajectory and the MI trajectory, respectively. Note how the MI trajectory resembles a square, but is distorted, particularly in the corners.

Figure 9(d) shows the recovered trajectory after using iMag method, which is virtually identical to the ground-truth and has corrected the odometry drift.

Table II shows that the e_{RMS} of IMU, MI and iMag methods are 4.527 m, 4.247 m and 0.752 m, respectively. Fusing measurements from MI and IMU, iMag can achieve 83.4% and 82.3% improvement compared with only using IMU and MI methods. Figure 9(e) shows the CDF of errors using different methods. The results show the 80th percentile localisation errors for IMU, MI and iMag are 6.1 m, 5.4 m, and 0.8 m. In this metric, iMag achieves 86.9% (compared with IMU method), 85.2% (compared with MI method) improvement.

D. Experiment 3: Random Walking

The goal of this experiment is to show the performance of our proposed method with a more realistic motion trace. This ground truth of this experiment is shown in Figure 10(a). The monitored person walks randomly, which leads to a 311.95 m path.

Figure 10(b) and Figure 10(c) demonstrate the IMU trajectory and the MI trajectory, respectively. Figure 10(d) shows the trajectory using iMag method.

Table III shows that the e_{RMS} of IMU, MI and iMag method are 3.491 m, 4.564 m and 2.453 m, respectively. Fusing measurements from MI and IMU, it can achieve a 29.7% and a 61.6% improvement compared with IMU and MI based localisation methods. Figure 10(e) shows the CDF of the different methods. The results show the 80th percentile localisation errors for IMU, MI and iMag methods are 4.8m, 6.2 m, and 2.5 m. With this metric, iMag achieves 47.9% (compared with IMU method) and a 59.7% (compared with MI method) improvement. This experiment demonstrates that even with long trajectories and sparse loop-closure points, iMag can accurately track users.

VI. CONCLUSIONS

In this paper, we proposed the iMag SLAM system and investigated its performance to meet the requirements of accurate localisation and rapid setup. A novel method of using low frequency magneto-inductive based positioning coupled with inertial measurements demonstrates excellent accuracy, irrespective of operating environment. Our prototype only needs one MI transmitter deployed in the area of interest, which allows for fast and easy setup, without any survey or calibration. Our evaluations show that our proposed method can achieve up to 86.9% and 85.2% improvement compared with using only an IMU or MI device for localisation.

VII. ACKNOWLEDGEMENTS

This work was supported by Innovate UK Tracksafe (Project 102033).

REFERENCES

[1] ALARP Track Warining Project. http://www.transport-research.info/project/railway-automatic-track-warning-system-based-distributed-personal-mobile-terminals. Accessed: 2016-03-29.

[2] Autoprowa Warning System. http://www.zoellner.de/en/. Accessed: 2016-03-29.

[3] Fast and Robust Curve Intersections. http://www.mathworks.com/matlabcentral/fileexchange/11837-fast-and-robust-curve-intersections/all_files. Accessed: 2016-03-29.

[4] GPS Accuracy. http://www.gps.gov/systems/gps/performance/accuracy/. Accessed: 2016-04-05.

[5] Rail Safety and Standards Board Annual Safety Performance Report 2013/14. http://www.rssb.co.uk/Library/risk-analysis-and-safety-reporting/2014-07-aspr-2013-14-full-report.pdf. Accessed: 2016-03-29.

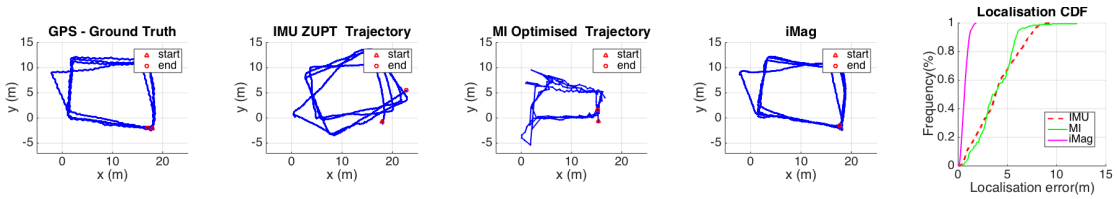

(a) Ground Truth (b) IMU (c) MI (d) iMag (e) cdf

Fig. 9. Experiment 2: Trajectories and CDF of walking in a regular path in an open outdoor environment

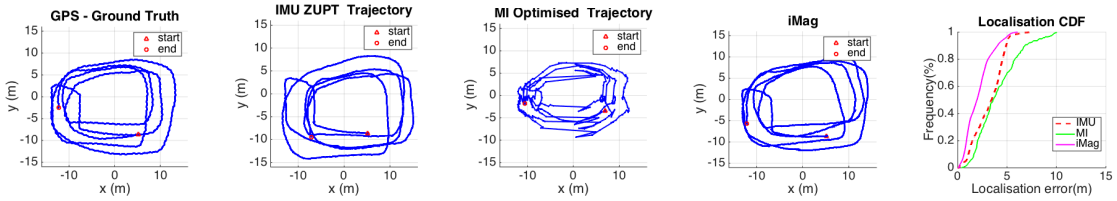

(a) Ground Truth (b) IMU (c) MI (d) iMag (e) cdf

Fig. 10. Experiment 3: Trajectories and CDF for random walking

[6] Rail Safety and Standards Board Annual Safety Performance Report 2014/15. http://www.rssb.co.uk/Library/risk-analysis-and-safety-reporting/2015-07-aspr-full-report-2014-15.pdf. Accessed: 2016-03-29.

[7] Xsens Gyroscopes. https://www.xsens.com/tags/gyroscopes/. Accessed: 2016-03-29.

[8] Xsens MTi 1-series module. https://www.xsens.com/products/mti-1-series/. Accessed: 2016-03-29.

[9] A Laser-Aided Inertial Navigation System (L-INS) for human localization in unknown indoor environments. *Proceedings - IEEE International Conference on Robotics and Automation*, pages 5376–5382, 2010.

[10] T. E. Abrudan, Z. Xiao, A. Markham, and N. Trigoni. Distortion Rejecting Magneto-Inductive Three-Dimensional Localization (MagLoc). *IEEE Journal on Selected Areas in Communications*, 33(11):2404–2417, 2015.

[11] G. Bellusci, D. Roetenberg, F. Dijkstra, H. Luinge, and P. Slycke. Xsens MVN MotionGrid : Drift-free human motion tracking using tightly coupled ultra-wideband and miniature inertial sensors. *Xsens Technologies White Paper*, pages 1–10, 2011.

[12] D. Bouvet and G. Garcia. Improving the accuracy of dynamic localization systems using RTK GPS by identifying the GPS latency. In *2000 IEEE International Conference on Robotics and Automation.*, volume 3, pages 2525–2530. IEEE.

[13] Chao Gao and R. Harle. Sequence-based magnetic loop closures for automated signal surveying. In *2015 International Conference on Indoor Positioning and Indoor Navigation (IPIN)*, pages 1–12. IEEE, oct 2015.

[14] F. Evennou and F. Marx. Advanced Integration of WiFi and Inertial Navigation Systems for Indoor Mobile Positioning. *EURASIP Journal on Advances in Signal Processing*, 2006:1–12, 2006.

[15] B. Ferris, D. Fox, and N. Lawrence. WiFi-SLAM using Gaussian process latent variable models, 2007.

[16] R. P. Feynman, R. B. Leighton, and M. Sands. *The feynman lectures on physics*. American Journal of Physics, 1965.

[17] J. Huang, D. Millman, M. Quigley, D. Stavens, S. Thrun, and A. Aggarwal. Efficient, generalized indoor WiFi GraphSLAM. *Proceedings - IEEE International Conference on Robotics and Automation*, pages 1038–1043, 2011.

[18] X. Jiang, C.-J. M. Liang, K. Chen, B. Zhang, J. Hsu, J. Liu, B. Cao, and F. Zhao. *Design and evaluation of a wireless magnetic-based proximity detection platform for indoor applications*. ACM, New York, New York, USA, Apr. 2012.

[19] A. R. Jimenez, F. Seco, J. C. Prieto, and J. Guevara. Indoor Pedestrian navigation using an INS/EKF framework for yaw drift reduction and a foot-mounted IMU. *Proceedings of the 2010 7th Workshop on Positioning, Navigation and Communication, WPNC'10*, pages 135–143, 2010.

[20] E. S. Jones and S. Soatto. Visual-inertial navigation, mapping and localization: A scalable real-time causal approach. *The International Journal of Robotics Research*, jan 2011.

[21] J. Jung, T. Oh, and H. Myung. Magnetic field constraints and sequence-based matching for indoor pose graph slam. *Robotics and Autonomous Systems*, 70:92–105, 2015.

[22] L. Klingbeil and T. Wark. A wireless sensor network for real-time indoor localisation and motion monitoring. In *Information Processing in Sensor Networks, 2008. IPSN'08. International Conference on*, pages 39–50. IEEE, 2008.

[23] R. Kummerle, G. Grisetti, H. Strasdat, K. Konolige, and W. Burgard. G2o: A general framework for graph optimization. In *2011 IEEE International Conference on Robotics and Automation*, pages 3607–3613. IEEE, may 2011.

[24] K. Lorincz, D. J. Malan, T. R. Fulford-Jones, A. Nawoj, A. Clavel, V. Shnayder, G. Mainland, M. Welsh, and S. Moulton. Sensor networks for emergency response: challenges and opportunities. *Pervasive Computing, IEEE*, 3(4):16–23, 2004.

[25] A. Markham, N. Trigoni, S. a. Ellwood, and D. W. Macdonald. Revealing the hidden lives of underground animals using magneto-inductive tracking. *Proceedings of the 8th ACM Conference on Embedded Networked Sensor Systems - SenSys '10*, (September):281, 2010.

[26] P. Mirowski, T. K. Ho, Saehoon Yi, and M. MacDonald. SignalSLAM: Simultaneous localization and mapping with mixed WiFi, Bluetooth, LTE and magnetic signals. In *International Conference on Indoor Positioning and Indoor Navigation*, pages 1–10. IEEE, oct 2013.

[27] S. Papaioannou, H. Wen, Z. Xiao, A. Markham, and N. Trigoni. Accurate Positioning via Cross-Modality Training. In *Proceedings of the 13th ACM Conference on Embedded Networked Sensor Systems - SenSys '15*, pages 239–251, New York, New York, USA, 2015. ACM Press.

[28] V. Pasku, A. De Angelis, M. Dionigi, G. De Angelis, A. Moschitta, and P. Carbone. A Positioning System Based on Low Frequency Magnetic Fields. *IEEE Transactions on Industrial Electronics*, 0046, 2015.

[29] G. Pirkl and P. Lukowicz. Robust, low cost indoor positioning using magnetic resonant coupling. In *Proceedings of the 2012 ACM Conference on Ubiquitous Computing - UbiComp '12*, page 431, New York, New York, USA, 2012. ACM Press.

[30] D. Roetenberg, H. Luinge, and P. Slycke. Xsens mvn: full 6dof human motion tracking using miniature inertial sensors. *Xsens Motion Technologies BV, Tech. Rep*, 2009.

[31] I. Vallivaara, J. Haverinen, A. Kemppainen, and J. Röning. Simultaneous localization and mapping using ambient magnetic field. In *Multisensor Fusion and Integration for Intelligent Systems (MFI), 2010 IEEE Conference on*, pages 14–19. IEEE, 2010.

[32] H. Wang, A. Elgohary, and R. R. Choudhury. No Need to War-Drive : Unsupervised Indoor Localization. *Proceedings of the 10th*

international conference on Mobile systems, applications, and services (MobiSys '12), pages 197–210, 2012.

[33] Z. Xiao, H. Wen, A. Markham, and N. Trigoni. *Lightweight map matching for indoor localisation using conditional random fields*. 2014.